Avaliação de um modelo empírico utilizado para derivar a velocidade de fluidização de misturas binárias de biomassa e areia

Evaluation of an empirical model used for deriving the fluidization velocity of binary mixtures of biomasses and sand

Evaluación de un modelo empírico utilizado para derivar la velocidad de fluidización de mezclas binarias de biomasas y arena

David da Silva Vasconcelos

ORCID: https://orcid.org/0000-0002-1878-6940

Universidade Federal da Bahia, Brasil

E-mail: david_stronda@hotmail.com

Sirlene Barbosa Lima

ORCID: https://orcid.org/0000-0002-8080-2040

Universidade Federal da Bahia, Brasil

E-mail: sirlenebl@gmail.com

Ana Cristina Morais da Silva

ORCID: https://orcid.org/0000-0002-3412-5990

Universidade Federal da Bahia, Brasil

E-mail: acristinasilva@ufba.br

José Mário Ferreira Júnior

ORCID: https://orcid.org/0000-0003-4295-6417

Universidade Federal da Bahia, Brasil

E-mail: jmfj@ufba.br

Carlos Augusto de Moraes Pires

ORCID: https://orcid.org/0000-0003-4231-6495

Universidade Federal da Bahia, Brasil

E-mail: cap@ufba.br

Resumo

Em um estudo anterior, um modelo estatístico foi desenvolvido usando a técnica de planejamento experimental para avaliar a influência de suas variáveis na velocidade de fluidização. Neste estudo, investigamos o modelo estatístico Vasconcelos (VSM) na

representação de dados, considerando a fluidização com e sem segregação. A metodologia utilizada foi baseada na simulação da velocidade de fluidização de nove sistemas binários, compreendendo areia e oito biomassas publicadas por seis autores. Além disso, os resultados obtidos com o VSM foram comparados com os obtidos com outros cinco modelos, relatados por diferentes autores, mas ajustados aos dados experimentais dessas biomassas. O resultado obtido pelos modelos propostos indicou principalmente uma discrepância entre as velocidades de fluidização experimental e calculada. O VSM, usando apenas três variáveis (tamanho de partícula, diâmetro de partícula e fração de massa de biomassa), produziu resultados de menores valores de discrepância em todas as simulações (2,23 a 12,51%), em oposição aos outros modelos comparativos, que apresentaram maior número de variáveis. Assim, o VSM é definido como um dos modelos mais interessantes para prever a velocidade de fluidização de várias biomassas.

Palavras-chave: Velocidade de fluidização; Mistura binária; Modelo empírico; Modelo estatístico.

Abstract

In a previous study, a statistical model was developed using the experimental planning technique for evaluating the influence of its variables on fluidization velocity. In this study, we investigated the Vasconcelos-statistical model (VSM) in data representation, considering fluidization with and without segregation. The methodology used was based on the simulation of the fluidization velocity of nine binary systems, comprising sand, and eight biomasses published by six authors. In addition, the results obtained using VSM were compared with those obtained using five other models, reported by different authors, but adjusted to the experimental data of these biomasses. The result obtained by the proposed models mainly indicated a discrepancy between the experimental and calculated fluidization velocities. VSM, using only three variables (particle size, particle diameter, and biomass mass fraction), yielded results of smaller discrepancy values in all simulations (2.23–12.51%), as opposed to the other comparative models, which presented more significant numbers of variables. Thus, VSM is defined as one of the most interesting models for predicting the fluidization velocity of several biomasses.

Keywords: Fluidization velocity; Mixture binary; Empirical model; Statistical model.

Resumen

En un estudio anterior, se desarrolló un modelo estadístico utilizando la técnica de planificación experimental para evaluar la influencia de sus variables en la velocidad de fluidización. En este estudio, investigamos el modelo estadístico de Vasconcelos (VSM) en la representación de datos, considerando la fluidización con y sin segregación. La metodología utilizada se basó en la simulación de la velocidad de fluidización de nueve sistemas binarios, que comprenden arena y ocho biomasas, publicados por seis autores. Además, los resultados obtenidos con el VSM se compararon con los obtenidos con otros cinco modelos, informados por diferentes autores, pero ajustados a los datos experimentales de estas biomasas. El resultado obtenido por los modelos propuestos indicó principalmente una discrepancia entre las velocidades de fluidización experimentales y calculadas. VSM, utilizando solo tres variables (tamaño de partícula, diámetro de partícula y fracción de masa de biomasa), produjo resultados de valores de discrepancia más bajos en todas las simulaciones (2.23 a 12.51%), en oposición a otros modelos comparativos, que presentaron un mayor número de variables. Por lo tanto, VSM se define como uno de los modelos más interesantes para predecir la velocidad de fluidización de varias biomasas.

Palabras clave: Velocidade de fluidização; Mistura binária; Modelo empírico; Modelo estatístico.

1. Introduction

Fluidization produces a uniform heat transfer, whose main effect is the maintenance of the fluidized bed reactor temperature at desired values, and consequently, better transformation of the biomass. For these reasons, the fluidization of binary systems has been widely used in pyrolysis, gasification, and combustion for a wide range of biomasses (Bridgewater, 2004; Jeong, Lee, Chang, & Jeong, 2016; Wang et al., 2016). Binary fluidization is considered more complex than the fluidization of a single material due to the possibility of particle segregation decrease the homogeneity of solid mixtures (Formisani & Girimonte, 2003).

Gas velocity is the main operational parameter of fluidization, ensuring that the mixture exhibits a behavior intermediate between those of a fixed fluidized bed reactor and the particulate flow. With the ideal gas velocity maintained, it is possible to obtain the velocity at which fluidization starts, called minimum fluidization velocity (Oliveira et al., 2013), for homogeneous mixing and the final fluidization velocity for segregated mixtures

(Formisani & Girimonte, 2003).

Several models have been developed to determine the minimum and final fluidization velocities. The minimum fluidization velocity is determined by considering the properties of the particles and fluidizing gases, diameters, and geometry of the fluidized bed reactor and design of the distributor (Yang, 2003). On the other hand, the final fluidization velocity is determined by considering the minimum fluidization velocity, properties of materials (such as densities and diameters of solids), the mass fraction of lighter components, minimum fluidity porosity, and reactor parameters (such as fluidized bed reactor height) (Formisani, Girimonte, & Vivacqua, 2013).

Vasconcelos et al. (2018) developed an equation for the final fluidization velocity of a binary mixture of the sisal residue (SR) and sand. They also successfully used this equation to identify the minimum fluidization velocity of corn cob (CC), walnut shell (WS), waste tobacco (WT), sweet sorghum bagasse (SB), and soybean hull (SH). Other models have been developed to identify the final velocity of fluidization; however, they were developed for mineral binary systems (Formisani, Girimonte, & Vivacqua, 2011; Formisani, Girimonte, & Vivacqua, 2013).

Wen and Yu (1966), Rao and Bheemarasetti (2001), Si and Guo (2008), Zhong et al. (2008), and Paudel and Feng (2013) developed the minimum fluidization velocity models based on particles' effective diameters and densities, density and viscosity of the fluidizing gas, and acceleration of gravity. The effective properties were evaluated from the solid diameter, solid density, and mixture composition. The model developed by Vasconcelos et al. (2018) used the same variables, without considering effective diameters and densities (Vasconcelos-dimensional model (VDM)).

From the viewpoint of the experimental planning technique, Vasconcelos et al. (2018) also developed an empirical model (Vasconcelos-statistical model (VSM)) to identify the influence of particle sizes and biomass mass fraction on the final fluidization velocity. Although they did not focus on evaluating this model concerning the pre-existing models and other biomasses, satisfactory predictions were obtained for a binary mixture of SR and sand. Besides, this model is considered attractive because it uses fewer variables compared to other models presented in the literature.

The previously proposed models were developed to predict fluidization velocity for a specific biomass type and conditions, obtaining satisfactory results. However, there is still no consensus regarding the best prediction model for the fluidization velocity (minimum or final) of a binary mixture that is independent of the biomass type and operating conditions.

The present study aims to investigate whether VSM, developed by Vasconcelos et al. (2018), can adequately predict the fluidization velocity (minimum and final) for any type of biomass or operational condition. The novelty of this study lies in the use of an empirical model, constructed and evaluated based on statistics and with only three variables (particle size, particle diameter, and biomass mass fraction), while the other models contain eight variables and have been proposed to determine the fluidization velocity under specific biomass and operation conditions.

2. Materials and Methods

2.1. Biomasses

This study was conducted using biomass data obtained from the literature, such as de Oliveira et al. (1913) (WT, WT*, SB, and SH), Vasconcelos et al. (2018) (SR), Zhong et al. (2008) (wood chip (WC) and mung bean (MB)), and Paudel and Feng (2013) (CC and WS); these biomasses were fluidized together with sand, whose properties are shown in Table 1.

Table 1 – Material properties.

Properties	WT	SB	SH	WT*	WC	MB	CC	WS	SR
	Oliveira et al. (2013)	Oliveira et al. (2013)	Oliveira et al. (2013)	Oliveira et al. (2013)	Zhong et al. (2008)	Zhong et al. (2008)	Paudel and Feng (2013)	Paudel and Feng (2013)	Vasconcelos et al. (2018)
d_{sand} (mm)	0.35	0.35	0.35	0.67 - 1.13	0.5 - 1.3	1.0	0.241	0.241	0.2 - 0.8
d_{bio} (mm)	0.25 - 0.6	0.25 - 0.65	0.3 - 0.8	0.25 - 0.26	0.89	3.2	1.04	0.856	0.2 - 0.8
W_{bio}	0.05 - 0.15	0.05 - 0.15	0.05 - 0.15	0.05 - 0.15	0 - 0.25	0 - 1	0 - 1	0 - 1	0.05 - 0.09
ρ_{sand} (kg.m^{-3})	2695.5	2695.5	2695.5	2695.5	2700	2700	2630	2630	2693.7
ρ_{bio} (kg.m^{-3})	1301.7 - 1431.4	1469.7 - 1498.9	1432 - 1448.8	1695.5	560	1640	1080	1200	1700.4
d_{bio}/d_{sand}	0.71; 1; 1.71	0.71; 1.14; 1.86	0.86; 1.71; 2.29	0.22; 0.29; 0.31; 0.37; 0.41; 0.52; 0.53; 0.70; 0.89	0.68; 0.89; 1.78	3.2	4.31	3.55	0.4; 0.43; 0.69; 1; 1.6; 2.33; 2.5
ρ_{bio}/ρ_{sand}	0.48 - 0.53	0.54 - 0.56	0.53	0.48 - 0.51	0.21	0.61	0.41	0.45	0.17 - 0.22
Geld. sand	B	B	B	D	D	D	B	B	B - D
Geld. bio	B	B	B	B	B	D	B	B	B
$\bar{\epsilon}_{mix}$	0.51	0.53	0.40	0.52	0.48	0.52	0.46	0.44	0.78

Source: Authors.

Table 1 shows some properties of the studied materials and mixtures, such as particle diameters (dsand and dbio), particle densities (ρsand and ρbio), mixture biomass fractions (Wbio), and porosity mixture average ($\bar{\epsilon}_{mix}$). It also shows the ratios between these properties and biomass, such as diameters (sand/biomass), densities (sand/biomass), and Geldart (Geld.) classification of materials.

The diameters were obtained using different procedures. Dynamic digital images were analyzed to determine the particle size and shape distributions in SB, WT, and SH samples. In contrast, the diameters of approximate sphere particles of WC and MB were measured using a

laser particle size analyzer (Mastersizer, 2000). The Sauter mean diameters of CC and WS were calculated, and the average particle length of SR was determined from that of the sieve openings that retained the material and the size immediately preceding it. Due to the use of different particle size identification techniques, this method is considered inaccurate in determining SR's particle size (Yang, 2003). However, the errors presented in particle size determination did not necessarily represent a problem for this study, because they contributed to improve prediction of the fluidization velocity prediction equations. This can be verified by comparing the predicted value of fluidization velocity with the experimental value for the various biomasses used here. Analyzing the properties of the fluidization components, it was verified that the sand and biomass diameters exhibit significant variations, of 0.2–1.3 mm and 0.2–3.2 mm, respectively.

The biomass mass fractions ranged from 0% to 100%, but most of them were in the range of 0%–25%. Although most biomass mass fractions involve a narrow range of values, only SR fractions have been justified by preliminary testing (Vasconcelos et al., 2018). The densities of sand have a narrow variation range (2630–2700 kg.m^{-3}), while the densities of the biomass have a larger variation range (560–1700.4 kg.m^{-3}). The ratios between the diameters of biomass and sand, and probably between the densities, produced stable and unstable mixtures, providing broader analyses of the model in the prediction of fluidization velocity (minimum and final). According to Chiba et al. (1979), homogeneous fluidization occurs when the ratio between the biomass and sand diameters is greater than 1.4142. Therefore, it can be considered that the fluidizations involving MB, WS, and CC were homogeneous, having dbio/dsand values of 3.2, 3.55, and 4.31, respectively.

On the other hand, WT* fluidization occurred with segregation in all tests, due to low dbio/dsand values (0.22–0.89). The Geldart classifications of individual materials were obtained from the biomass and sand evaluated by Oliveira et al. (1913). The Geldart classification for fluidization systems analyzed by other authors was determined from the densities and particle diameters provided by them. The Geldart classification is obtained by subtracting the density between a particle and air ($\rho_{particle} - \rho_{ar}$), as a function of particle diameter (Yang, 2003). The Geldarte B classification is defined for the sand particles and some biomasses (WT, SB, SH, CC, and WS) that participated in the same tests. This classification indicates that the materials fluidized satisfactorily under the action of vigorous bubbles, presenting moderate solid mixtures. In other situations as well, such as WT*, WC, and SR fluidization, the biomasses were Geldart B-rated, but the sands that fluidized with

these biomasses were rated D. In this case, the D rating indicates that the fluidization involves large particles and a low solid mixture. The binary fluidization with Geldarte D and B of sand and biomass, respectively, must have had some sort of segregation. The fluidization that should present the highest segregation is the sand and Mung bean mixture, due to the Geldart D classification of both materials. However, the ratio between the diameters was very high (3.2), which is characteristic of homogeneous fluidization.

The average porosity of the beds was obtained directly from the literature in the case of WT, SB, and SH (Oliveira et al., 1913), and was calculated from the density and bulk density in the case of WC, MB, CC, WS, and SR (Yang, 2003). The average porosity for all biomasses analyzed in this study ranged from 0.4 to 0.78, whose lowest value corresponds to that of SH and the highest value corresponds to that of SR. According to Cluet et al. (2015), an increase in the biomass mass fraction increases the porosity; however, in the case of SR, the smallest mass fraction produced the largest porosity. An explanation for this discrepancy is that SR particles are saddle-shaped, increasing the porosity of the sand mixture.

2.2. Models

The prediction velocity fluidization models (minimum and final) used in this study were analyzed by Vasconcelos et al. (2018). These authors reported the characteristics of the models developed by Oliveira et al. (2013), Paudel and Feng (2013), Zhong et al. (2008), and Si and Guo (2008), besides presenting two new models. These models were named Oliveira model (OM), Paudel model (PM), Zhong model (ZM), and Si model (SM), and those developed by Vasconcelos et al. (2018) were named VSM and VDM. All these models were used to predict the fluidization velocity of homogeneous and non-homogeneous systems, which makes them robust for applications. The models, as well as the biomasses used in the original studies, are shown in Table 2.

VDM and VSM were based on dimensionless analysis and statistical design of experiments, respectively. VDM was developed to find an equation that provides a more accurate prediction than the literature models for the final fluidization velocity of the mixture between sand and SR. This was necessary due to the difficulty of fluidization of this biomass by its unique saddle shape. This model provided excellent prediction results for mixtures with high and low dbio/dsand values and different particle geometries. VSM was developed using the experiment design technique to evaluate the influence of particle diameter and biomass mass fraction, as well as their interactions, on the final velocity of sand fluidization with sisal

residue. The predictions presented for SR by VSM were as good as those presented by the VDM model. Theoretically, this model would be limited to the ranges of operational variables of SR fluidization (biomass and sand diameters and biomass mass fraction); however, this study provided a new dimension to this empirical model by considering it for other biomasses.

The model developed by Oliveira et al. (2013) was applied to biomass with different particle sizes and densities. The relative error presented in the biomass and sand fluidization was 17.4% for biomasses with dbio/dsand value characteristic of a homogeneous and a non-homogeneous system (Vasconcelos et al., 2018). Paudel and Feng (2013) modified the Si and Guo (2008) equation, replacing the C2 coefficient, which is a function of sphericity, by the function that involves the sand and biomass mass fractions. PM was used to predict the fluidization velocity of homogeneous and non-homogeneous mixtures. In the original studies of these authors, the mixtures of CC and walnut shell with sand had dbio/dsand values of 4.31 and 3.55, respectively, which is characteristic of homogeneous mixtures. However, when this model was used to predict the final fluidization velocity of sand SR, which had inhomogeneous system characteristics, good results were obtained (Vasconcelos et al., 2018).

Table 2 – Model characteristics.

Reference	Model	Bed	Parameter
Vasconcelos et al. (2018) (VDM)	$Re_{ff}^* = A[B + D\,Ar^{*C3}]$ $Re_{ff}^* = \dfrac{\rho_f\, u_{ff}\, d_{sand}}{\mu}$ $Ar^* = \dfrac{d_{sand}^3\, \rho_f\, \rho_{bio}\, g}{\mu^2}$ $A = \dfrac{\rho_f}{\rho_{bio}}$ $B = C1\,\dfrac{\rho_{sand}}{\rho_{bio}}\dfrac{d_{bio}}{d_{sand}} + C4 + C5\,w_{bio}$ $D = C2\,A^{1-C3}$	Sisal residue (SR) Corn cob (CC) Walnut shell (WS) Waste tobacco	C1, C2, C3, C4, C5
Vasconcelos et al. (2018) (VSM)	$U_{ff} = C1 + C2\,W_{bio} + C3\,d_{bio} + C4\,d_{bio}^2 + C5\,d_{sand} + C6\,d_{sand}^2 + C7\,W_{bio}\,d_{sand} + C8\,d_{bio}\,d_{sand}$	Sisal residue (SR)	C1, C2, C3, C4, C5, C6, C7, C8
Oliveira et al. (2013) (OM)	$u_{mf} = C_1 \left[\dfrac{dp_{eff}^2(\rho_{eff} - \rho_f)g}{\mu_f}\left(\dfrac{\rho_{eff}}{\rho_f}\right)^{C_2}\right]^{C_3}$ $dp_{eff} = d_{sand}\left[\left(\dfrac{\rho_{sand}}{\rho_{bio}}\right)\left(\dfrac{d_{bio}}{d_{sand}}\right)\right]^{w_{sand}/w_{bio}}$ $\rho_{eff} = \dfrac{w_{sand}\rho_{sand} + w_{bio}\rho_{bio}}{w_{sand} + w_{bio}}$	Waste tobacco (WT) Sweet sorghum bagasse (SB) Soybean hulls (SH) Waste tobacco (WT*) Silica Sand	C1, C2, C3

Paudel and Feng (2013) (PM)	$$u_{mf} = \frac{\mu}{dp_{eff}\,\rho_f}\left\{\left[C_1{}^2 + H\frac{dp_{eff}{}^3\rho_f(\rho_{eff}-\rho_f)g}{\mu^2}\right]^{C_5} - C_1\right\}$$ $$H = C_2\,w_{sand} + C_3\,w_{bio}{}^{C_4}$$ $$dp_{eff} = d_{bio}\,d_{sand}\left[\frac{w_{bio}\rho_{sand} + w_{sand}\rho_{bio}}{w_{bio}\rho_{sand}d_{sand} + w_{sand}\rho_{bio}d_{bio}}\right]$$ $$\rho_{eff} = \frac{\rho_{bio}\,\rho_{sand}}{w_{sand}\rho_{bio} + w_{bio}\rho_{sand}}$$	Corn cob (CC) Walnut shell (WS) Silica Sand Glass beads Alumina	C1, C2, C3, C4
Zhong et al. (2008) (ZM)	$$u_{mf} = C_1\left[\frac{dp_{eff}{}^2(\rho_{eff}-\rho_f)g}{\mu}\left(\frac{\rho_{eff}}{\rho_f}\right)^{1.23}\right]^{C_2}$$ $$dp_{eff} = d_{sand}\left[\left(\frac{\rho_{sand}}{\rho_{bio}}\right)\left(\frac{d_{bio}}{d_{sand}}\right)\right]^{w_{sand}/w_{bio}}$$ $$\rho_{eff} = w_{sand}\rho_{sand} + w_{bio}\rho_{bio}$$	Wood chip (WC) Mung bean (MB) Millet Corn stalk Coton stalk Silica sand Continental flood basalt cinder Aluminum oxide	C1, C2
Si and Guo (2008) (SM)	$$u_{mf} = \frac{\mu}{dp_{eff}\,\rho_f}\left\{\left[C_1{}^2 + C_2\frac{dp_{eff}{}^3\rho_f(\rho_{eff}-\rho_f)g}{\mu^2}\right]^{C_3} - C_1\right\}$$ $$dp_{eff} = d_{bio}\,d_{sand}\left[\frac{w_{bio}\rho_{sand} + w_{sand}\rho_{bio}}{w_{bio}\rho_{sand}d_{sand} + w_{sand}\rho_{bio}d_{bio}}\right]$$ $$\rho_{eff} = w_{sand}\rho_{sand} + w_{bio}\rho_{bio}$$	Sawdust Wheat stalk Quartiz sand	C1, C2, C3

Source: Authors.

The model of Zhong et al. (2008) was developed to predict the minimum fluidization velocity of different biomasses and fluidizing media. This study was based on the general expression proposed by Coltters and Rivas (2004), and proposed equations for effective densities below 1000 kg.m^{-3} and above this value. The predictions made by ZM involved high and low dbio/dsand values, producing a relative error of 14.7% (Zhong et al., 2008). When used for SR, under more severe fluidization conditions, the relative error was 20.73% (Vasconcelos et al., 2018). The Si and Guo (2008) model was developed to predict minimum fluidization velocities of binary mixtures with different particle sizes and densities. These authors adapted Wen and Yu's (1966) equation to include sphericity and effective particle size and density. The fluidization presented in their study was homogeneous, a fact the high dbio/dsand value predicted that.

2.3. Parameter regression

The parameter regressions of the presented model were divided into two steps: (i) to predict the minimum fluidization velocity (Table 3), denominated single regression, and (ii) the minimum and final fluidization velocities for the specific biomass, denominated individual regressions.

i) was achieved using WT, WT*, SB, and SH data to find a single equation from a single set of parameter values.

ii) was achieved using individual data from each biomass (specific biomass) to find the parameter value velocities (Table 4).

The parameters of the fluidization velocity model (minimum and final) were adjusted using nonlinear regression methods, such as quasi-Newton method, Hooke–Jeeves pattern moves, and Rosenbrock pattern search. The fluidization velocity models (Table 2) were adjusted from the regression methods cited; however, Tables 3 and 4 represent only the parameter sets related to the adequate adjustments, regardless of the optimization method used.

Table 3 - Correlation parameters – single regression for WT, SB, and SH.

Reference	Model	Parameter							
		C1	C2	C3	C4	C5	C6	C7	C8
Oliveira et al. (2013)	OM	3.02×10^{-9}	3.89	0.53					
Zhong et al. (2008)	ZM	2.40×10^{-5}	0.57						
Paudel and Feng (2013)	PM	5.75	6.25×10^{5}	6.05×10^{7}	2.11	9.67×10^{-2}			
Si and Guo (2008)	SM	-0.81	2.52×10^{-4}	1.33					
Vasconcelos et al. (2018)	VDM	5.00	8.34×10^{4}	0.29	-4.77×10^{3}	-200.0			
Vasconcelos et al. (2018)	VSM	0.07	-4.00×10^{-4}	114.00	0.13	2.1×10^{5}	-1.6×10^{5}	0.24	-250.87

Source: Authors.

Table 4 - Correlation parameters – individual parameter regression for each biomass.

Reference	Model	Biomass	Parameter							
			C1	C2	C3	C4	C5	C6	C7	C8
Oliveira et al. (2013)	OM	WT	1.70×10^{-3}	0.31	0.79					
		SB	2.62	3.32	0.11					
		SH	3.00	-32.64	13.81×10^{-3}					
		WT*	4.00×10^{-5}	-5.99	-0.21					
		WC	1.49×10^{9}	-7.20	0.45					
		MB	9.13	90.91	-3.57×10^{-3}					
		CC	15.88×10^{3}	-102.09	9.22×10^{-3}					
		WS	19.07×10^{3}	-102.75	9.40×10^{-3}					
		SR	1.67	-1.63	0.21					
Zhong et al. (2008)	ZM	WT	2.26×10^{-7}	0.90						
		SB	0.79	-0.14						
		SH	2.85×10^{-2}	8.52×10^{-2}						
		WT*	0.15	4.99×10^{-2}						
		WC	0.14	0.09						
		MB	1.21	-2.75×10^{-2}						
		CC	16.30	2.23×10^{-2}						
		WS	13.23	2.80×10^{-2}						
		SR	0.15	8.37×10^{-2}						
Paudel and Feng (2013)	PM	WT	915.08	-0.53	2.17	0.14	0.50			
		SB	8.74×10^{-2}	1.35	0.22	0.24	0.10			
		SH	-1.38	4.53×10^{-4}	7.06	4.51	0.12			
		WT*	23.30	171.01	10.30×10^{6}	6.75	0.24			
		WC	632.37	0.35	4.94	1.18	0.50			
		MB	103.84	75.43	68.76	6.69×10^{-2}	0.30			
		CC	9.40	1.60	729.00	-1.05	-2.69×10^{-2}			
		WS	10.02	0.44	537.65	0.53	-0.75			
		SR	-1.67	-4.03×10^{-3}	1.01×10^{-2}	4.24×10^{-2}	0.64			
Si and Guo	SM	WT	573.37	0.60	0.50					

Reference	Model	Param								
(2008)		SB	-6.88×10^{-2}	5.95×10^{-3}	0.25					
		SH	0.11	3.33×10^{-3}	0.34					
		WT*	41.93	22.20×10^{4}	0.18					
		WC	65.13	86.80×10^{4}	0.19					
		MB	-2.12	7.34×10^{-3}	0.56					
		CC	40.61	0.13	0.49					
		WS	60.48	0.22	0.50					
		SR	-1.79	3.74×10^{-3}	0.68					
Vasconcelos et al. (2018)	VDM	WT	84.22	174.26	3666.66	2632.63	0.39			
		SB	-59.12	-10.80	682.04	10.78	0.85			
		SH	-66.92	-3.39	2338.40	12.75	0.84			
		WT*	5191.86	-6696.2	-21.10×10^{3}	50.55	0.72			
		WC	10.09	44.22	15.09×10^{3}	89.10	0.71			
		MB	590.86	112.23	33.23×10^{3}	17.50	0.84			
		CC	9.40	1.60	729.00	-1.05	-2.69×10^{-2}			
		WS	10.02	0.44	537.65	0.53	-0.75			
		SR	-1408.0	40.00	0.80	13.89×10^{3}	-36.00×10^{3}			
Vasconcelos et al. (2018)	VSM	WT	7.00×10^{-2}	3.00×10^{-3}	60.00	0.27	1.48×10^{-4}	7.27×10^{-3}	0.12	0.40
		SB	0.11	-0.30	1.00×10^{-4}	3.00×10^{-6}	1.85×10^{-3}	-46.03×10^{3}	9.18×10^{-2}	1.57
		SH	9.70×10^{-2}	3.28×10^{-2}	-9.90×10^{-4}	0.11	0.10	-16.12×10^{3}	7.08×10^{-2}	9.42×10^{-2}
		WT*	-0.19	1008.00	108.50	0.43	-65.23×10^{4}	-58.90×10^{4}	71.50×10^{4}	-905.00
		WC	0.17	215.51	1.39	0.48	14.83×10^{4}	0.21	7.62×10^{-2}	45.90
		MB	0.61	0.10	0.10	0.37	0.10	0.10	0.10	0.10
		CC	7.32	0.42	0.64	53.40	0.10	0.16	0.11	1.48
		WS	5.96	9.15×10^{-4}	0.50	48.00	2014.00	1.00	9.41×10^{-3}	1.95×10^{-3}
		SR	1.65	-2.13	-1.73	-9.31	1.02	0.91	1.19	15.83

Source: Authors.

The quasi-Newton method is a nonlinear estimation procedure that evaluates the function at different points in each step, to estimate the first- and second-order derivatives. It requires that the objective function gradient be provided in each interaction. Sequentially, this

information is used to follow a path to the minimum of the loss function. The loss function represents a selected measure of discrepancy between the observed and predicted data by using the adjusted function (Broyden, 1967).

The Hooke–Jeeves pattern moves method is a nonlinear estimation technique used to minimize an unrestricted objective function and does not need to calculate the gradient and the matrix Hessian as other optimization methods. This technique estimates the probable direction of the extreme from a starting point and progresses in the presumable direction of the extreme as the value of the objective function decreases. This method is generally quite effective and used when the quasi-Newton method fails to produce estimates (Hooke and Jeeves, 1961).

The Rosenbrock pattern search method is a multivariate search method similar to the exploration phase of the Hooke–Jeeves method. However, instead of continuously exploring in the directions of the coordinate axes, new orthogonal directions are constructed using the Gram–Schmidt procedure, based on the sizes of the steps in the successful directions (Rosenbrock, 1960).

2.4. Discrepancy and dispersion

The discrepancy (φ) between the fluidization velocity predicted by the model ($u_{f\,(CALC)}$) and experimental ($u_{f\,(EXP)}$) was calculated from Eq. (1). The displayed value was absolute (ABS).

$$\varphi\ (\%) = \frac{100\ \text{ABS}(u_{f\,(EXP)} - u_{f\,(CALC)})}{u_{f\,(EXP)}}$$

$$(1)$$

Where $\delta\ (\%)$ is the average discrepancy considering all tests of a specific biomass.

The limits of the fluidization velocity dispersion values considered in this study were obtained from the positive and negative percentage variations of the experimental fluidization velocities.

3. Results

3.1. Parameter regressions – single and individual

The first step of this study aimed at evaluating the fit quality of the models,

considering two scenarios: a) each model was adjusted only once with the fluidization data of all biomasses (single regression), and b) each model was adjusted for each type of biomass (individual regression). To perform this step, the data provided by Oliveira et al. (2013), as well as OM, PM, ZM, SM, VSM, and VDM, were used.

Oliveira et al. (2013) simulated the minimum fluidization velocity of a set of binary systems: sand/WT and WT*, SB, and SH. They used a single equation, whose parameters were obtained from a dataset involving all biomasses (single regression). However, there is still no discussion in the literature that supports the parameter regression conducted by Oliveira et al. (2013), as intuitively, the regression of parameters using data from a single biomass seems more appropriate to define a fluidization velocity prediction equation. The parameters that provided the best adjustment results for the single regression are shown in Table 3 and those for the individual regression are shown in Table 4.

The average discrepancy values presented by each fluidization velocity model for the regression of a dataset and individual biomasses provided by Oliveira et al. (2013), are shown in Figure 1. It is observed that all models used provided smaller discrepancy values when the parameter regressions were conducted for each biomass.

The discrepancy values obtained for WT from the models studied are shown in Figure 1(a). The smallest discrepancy values for a single regression were obtained from SM, although PM, VSM, and ZM showed low discrepancy values. For the individual parameter regression, most of the models showed very close discrepancy values, below 6.31%, while SM showed the highest value.

It is observed that SM obtained discrepancy values from a single regression similar to that obtained from the individual regression. The model most sensitive to the variation of the data used in the regression (single or individual regression) was VDM, which exhibited a reduction of 18.62% in the discrepancy values when individual regression was performed.

The discrepancy values obtained for SB from the models studied are shown in Figure 1(b). For this biomass, the models most sensitive to the variation of data generated in the regression were SM (17.16%), PM (16.18%), and VSM (9.25%). Although all models produced discrepancy values below 6.08%, VSM generated the lowest value (4%).

The discrepancy values obtained for SH from the models studied are shown in Figure 1(c). The data obtained from this biomass produced two of the largest differences between the discrepancy values from single and individual regressions: 39.11% (VDM) and 19.7% (SM). Besides, these biomass data produced discrepancy values below 5.5% for all models whose parameters were obtained with individual regression; VSM, with 2.6% discrepancy; and

VDM, with 2.83% discrepancy.

The discrepancy values obtained for WT* from the models studied are shown in Figure 1(d). The data used to determine the discrepancy values of Figure 1(a) differed from those used to determine the discrepancy values of Figure 1(d) concerning the sand diameter and biomass density (Table 1). When Figure 1(a) considers a sand diameter of 0.35 mm and a density of 1301.7 kg.m^{-3} at 1431.4 kg.m^{-3}, Figure 1(d) considers a sand diameter of 0.67–1.13 mm and a density of 1695.5 kg.m^{-3}. The difference between the material properties contributed to the largest discrepancy values among the biomasses investigated at this stage of evaluation, which ranged from 10.89% to 69.30%. The difference in the discrepancy values between the single and individual regressions reached 54.35% (PM) and 36.86% (SM). These biomass data produced minimum discrepancy values of 14.81% (SM) and 10.89% (VSM), which are higher than the smaller discrepancy values produced using other biomasses.

A reduction in the discrepancy values between the predictions of the models that had parameter regression from data of a single regression biomass and from data of each biomass (individual regression) occurred for all biomasses. However, SM and VDM presented opposite results for WT and WT*, although the variations between their discrepancies were small (-0.23 and -2.11, respectively). When the adjustment of the model parameters was performed from a biomass dataset, the final equation produced high prediction errors due to the wide range of data that characterized the materials and binary mixture used (Table 1). On the other hand, when the regression was performed with specific biomass data that were desired to predict the fluidization velocity, the parameters adjusted to a specific experimental condition and produced results with low discrepancy. Figure 1 shows that the reduction in the discrepancy between the two cases studied depends on both the models and type of biomass; there are no design and material and blend characteristics that best characterize the reduction in discrepancy.

Figure 1 - Minimum fluidization velocity discrepancy between single and individual regressions. Predictions were made for the following biomasses: (a) WT, (b) SB, (c) SH, and (d) WT*.

(d)

(c)
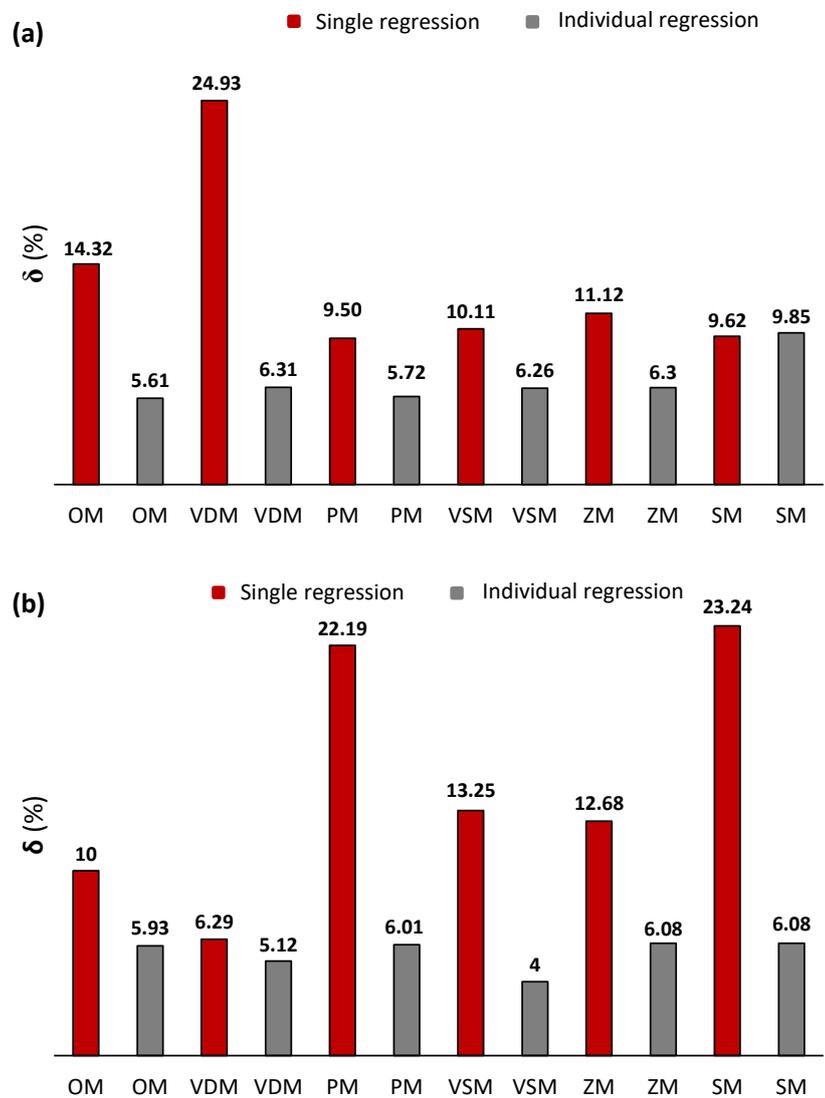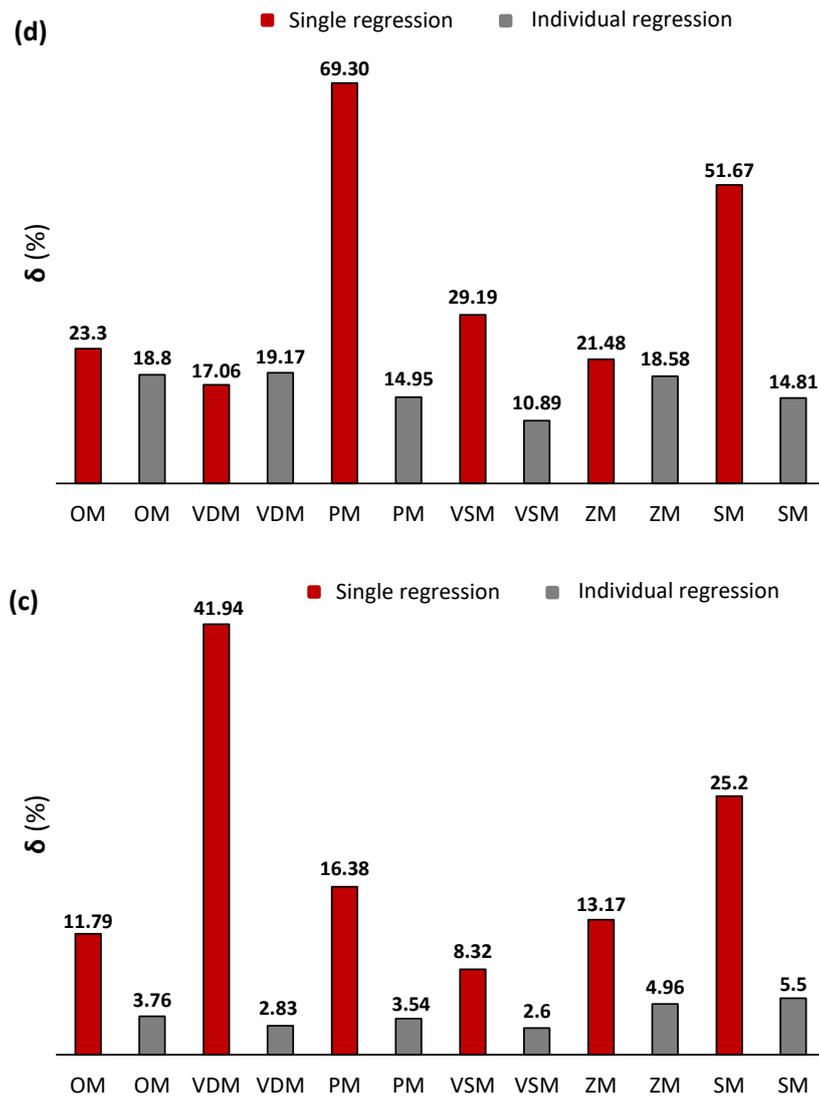
Source: Authors.

3.2. Evaluation of model

According to the previous item, the individual regression provided the lowest discrepancy values for the binary fluidization of sand with WT, WT*, SB, and SH. In the next items, the models were evaluated from nine biomasses with distinct characteristics (Table 1), all of which were defined based on the individual parameter regression of VSM, VDM, SM, PM, ZM, and OM. The simulations were performed, and the calculated minimum fluidization velocity values were compared with the experimental fluidization velocities for each type of biomass and model (Figs. 2–9). In the case of SR (Figure 10), the simulation responses refer to the final fluidization velocity due to adjustment of the nomenclature inherent in the segregated mixtures (Vasconcelos et al., 2018).

The results of the minimum fluidization velocity for WT, WT*, SB, and SH with sand are shown in Figs. 2–5, respectively. The experimental minimum fluidization velocities were obtained from the data presented in Oliveira et al.'s (2013) model. The dispersion values of the fluidization velocity computed comparatively to those of dispersion of the experimental fluidization velocity were mostly below 10%, as shown in Figs. 2–4, regardless of the model used. However, the dispersion values shown in Figure 5 were higher, despite being the same biomass as that assigned in Figure 2. The difference in the behavior of the fluidization velocity dispersion shown between Figs. 2 and 5 is probably related to the particle size of the sand, as the particle sizes of WT* fall within the range of WT. The ratio of biomass to sand diameters for the tests in Figure 2 ranged from 0.71 to 1.71 (Table 1), approaching the condition of homogeneous fluidization, which is greater than 1.4142. On the other hand, the ratios between the diameters for the tests in Figure 5 were longer than the homogeneous fluidization condition, as they presented values between 0.22 and 0.89 (Table 1). The biomass density was 1695.5 kg.m–3 for the tests in Figure 5 and 1301.7–1431.4 kg.m^{-3} for those in Figure 2 (Table 1), with the ratio of biomass to sand density ranging from 0.48 to 0.51 and 0.48 to 0.53, respectively. The similarity between the ratios involving the densities initially discarded this variable as a variation factor of fluidization velocity dispersion. Despite the high dispersion values shown in Figure 5, PM, and VSM presented the smallest average discrepancies (Figure 1). At low dispersion (Figs. 2–4), all models produced discrepancies below 7% (Figure 1). These results preliminarily indicate that PM and VSM can adequately represent the fluidization velocity in situations that also involve the segregation of components, making them more robust about the other models studied.

Figure 2 - Experimental versus calculated minimum fluidization velocity for WT and sand mixtures.
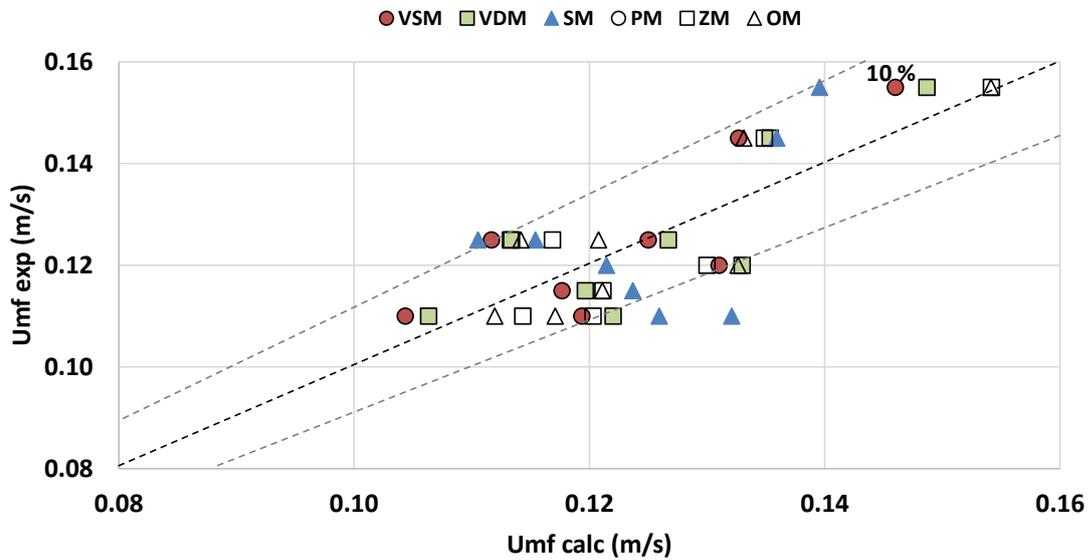
Source: Authors

Figure 3 - Experimental versus calculated minimum fluidization velocity for SB and sand mixtures.
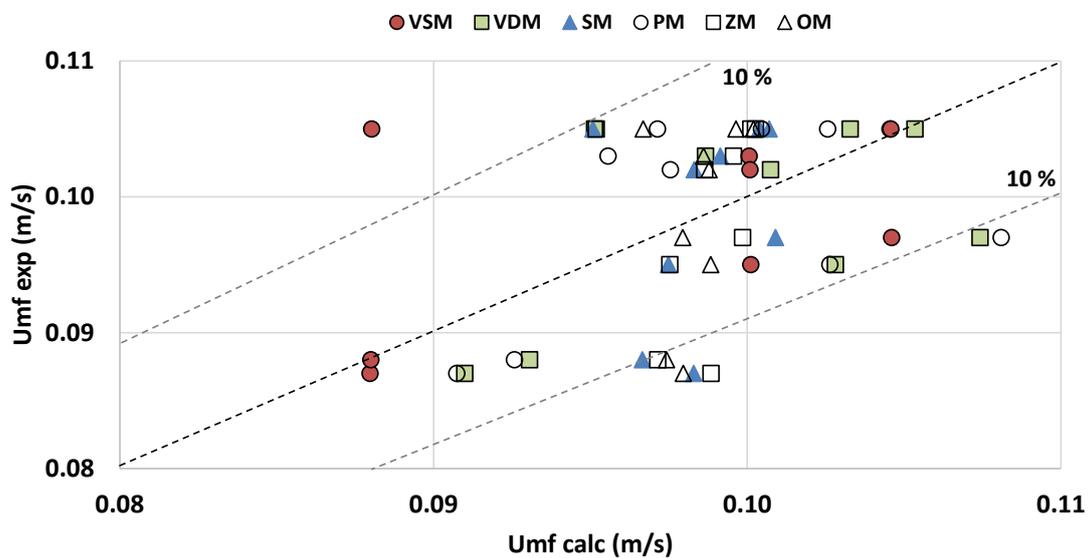
Source: Authors.

Figure 4 - Experimental versus calculated minimum fluidization velocity for SH and sand mixtures.
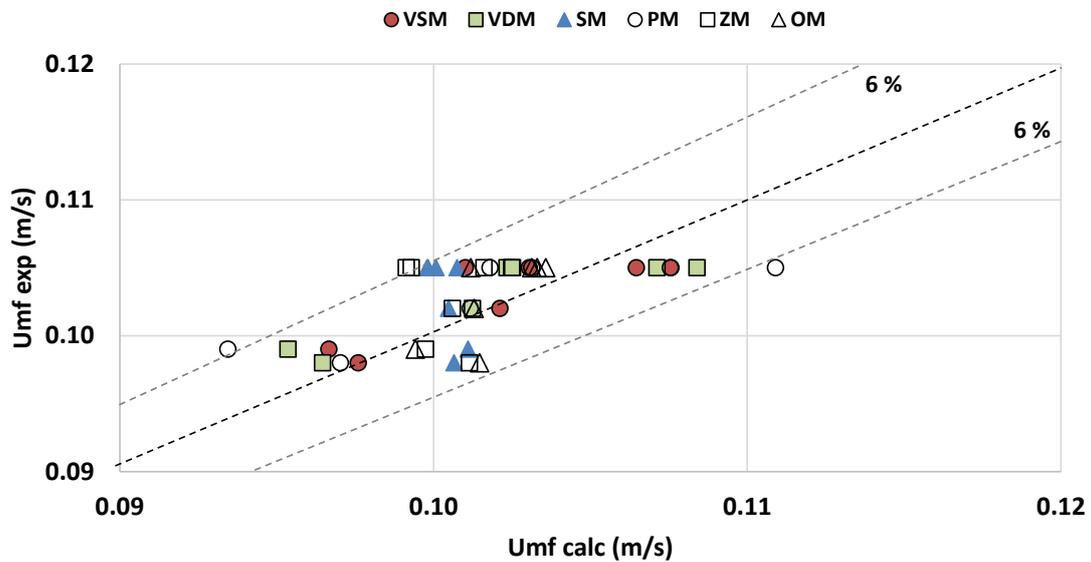
Source: Authors.

Figure 5 - Experimental versus calculated minimum fluidization velocity for WT* and sand mixtures.
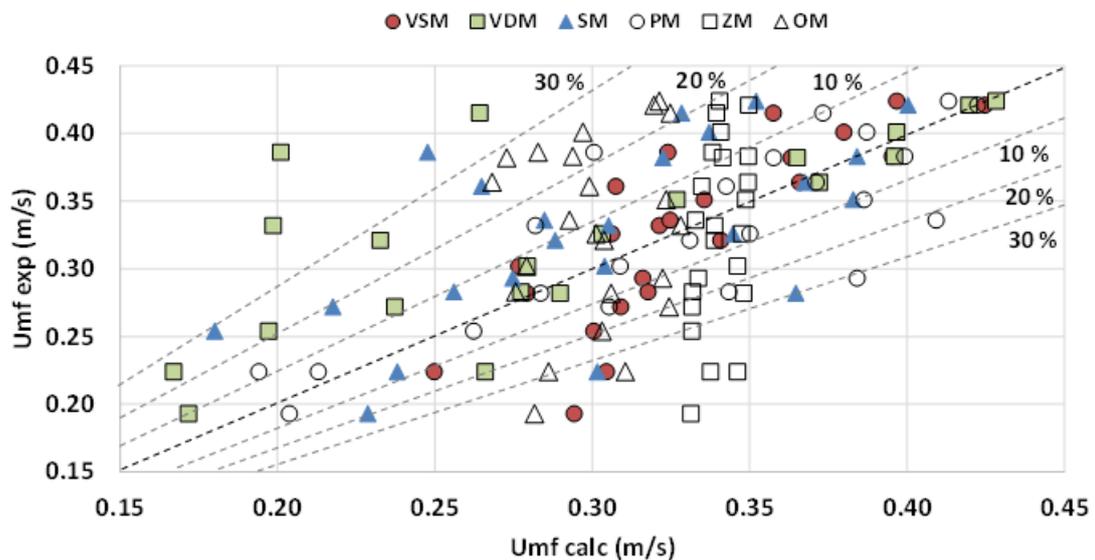
Source: Authors.

The dispersions values shown in Figs. 6–10 were based on the experimental fluidization rates of WC, MB, CC, WS, and SR, respectively. The scattering of the dispersion levels based on these figures followed the same logic as that attributed to the analyses

conducted for Figs. 2–5. Larger dispersion values were found for the smaller ratios between biomass and sand diameters. This is the case of Figs. 6 and 10, which showed ratios between 0.68 and 1.78 for the tests in Figure 6 and 0.4 and 2.5 for those in Figure 10. These reasons seem to be contradictory when verifying the values above the reference of a fluidized bed reactor considered homogeneous (>1.4142).

In case of WC (Figure 6), the only dbio/dsand value that reached the stability zone of the mixture was 1.78; however, there were two more reasons (0.68 and 0.89) that are below this zone and responsible for the dispersion. The balance of the effects between the smaller and larger ratio values produced smaller dispersion values than those presented in Figure 5. VSM and VDM presented dispersion values smaller than 10%.

In the case of SR (Figure 10), three ratios reached the zone of the homogeneous mixture (1.6, 2.33, and 2.5), while four did not reach (0.4, 0.43, 0.69, and 1.0), making interpretation difficult. As the obtained ratios were well above the initial zone of the homogeneous mixture, it can be assumed that the dispersion values were lower than those shown in Figure 6. However, the dispersion values were much higher and quite similar to those shown in Figure 5. The low ratio values between the diameters of the materials cannot be the only explanation for the high dispersion of the sand mixture with SR. An essential part of the explanation of the high dispersion observed must be attributed to the physical characteristics of the particle, discussed previously (Vasconcelos et al., 2018). SR particles have a saddle shape, which retains sand in their cavity and makes the material mixture unstable. This situation was minimized by limiting the biomass fraction between 5% and 8%; however, segregation still played an important role, contributing to increased dispersion due to particle shape. Figure 10 shows that all models had high dispersion values; however, the smallest dispersion values were attributable to VDM and VSM.

Figs. 7–9 present dispersion values between 10% and 20%; however, most of the models presented dispersion values below 10%. ZM is an exception to this behavior, which can be explained by comparing it with OM, due to the similarity between them. The difference between these models lies in the exponent related to the ratio between effective density and fluid density. The exponent between densities is a regression parameter for OM (C2) and a fixed value for ZM (1.23). They exhibited similar performances in the simulations presented in Figure 7; however, OM performed better in the simulations presented in Figs. 8 and 9. The similar performance of the two models (Figure 7) also occurred with WT* (Figure 1(d)), with the behavioral pattern attributed to the material segregation being observed. In this case, the ratios between biomass and sand diameters were mostly in the inhomogeneous

mixing range, which is also justified with Geldart D for sand and B for biomass. Another important observation that justifies the similarity of performance of the two models in terms of fluidization of the WT and WC sand mixture is their lack of sensitivity when parameter C2 is in the range of 3.32 to -32.64, which includes the ZM exponent equivalent to this parameter (1.23). ZM performed worse than OM in the simulations shown in Figs. 8 and 9; ZM continued with low sensitivity because of the exponent 1.23, while OM better adjusted to the experimental data considering parameter C2 being lower than -32.64. Very low parameter values were found in a very homogeneous mixing situation determined by the ratios between diameters greater than 3.2 (Table 1).

Figure 6 - Experimental versus calculated minimum fluidization velocity for WC and sand mixtures.
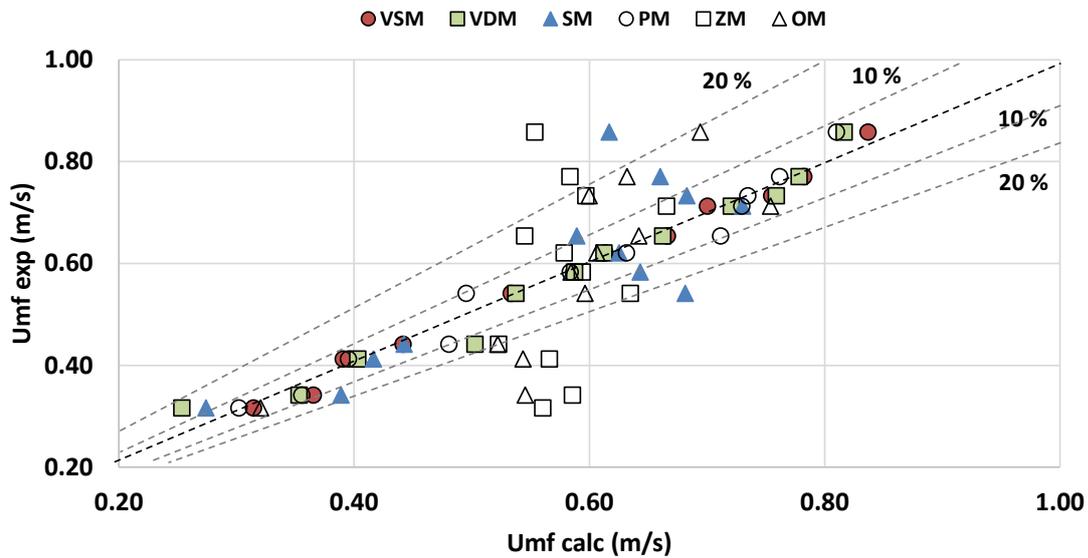
Source: Authors.

Figure 7 - Experimental versus calculated minimum fluidization velocity for MB and sand mixtures.
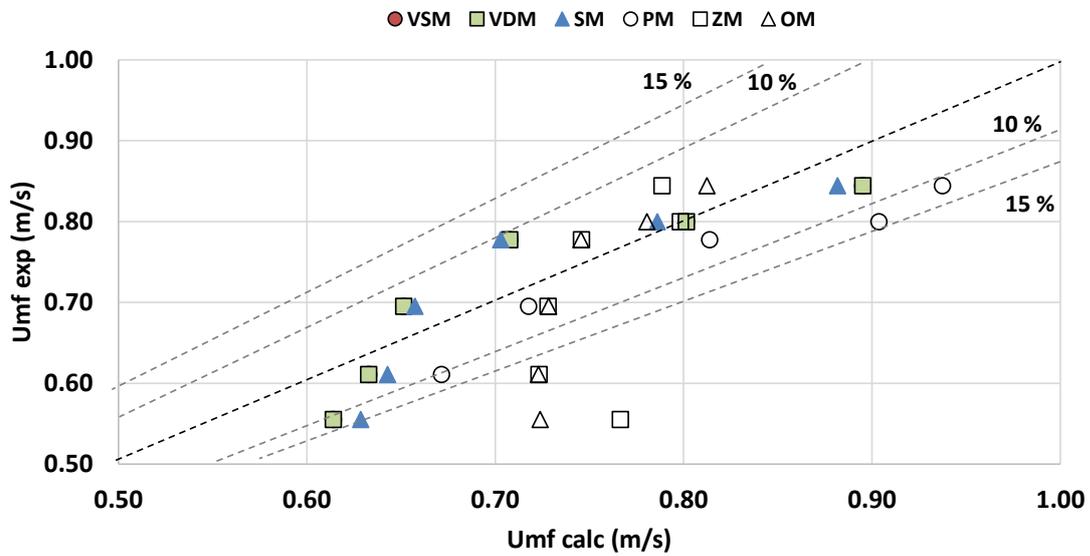
Source: Authors.

Figure 8 - Experimental versus calculated minimum fluidization velocity for CC and sand mixtures.
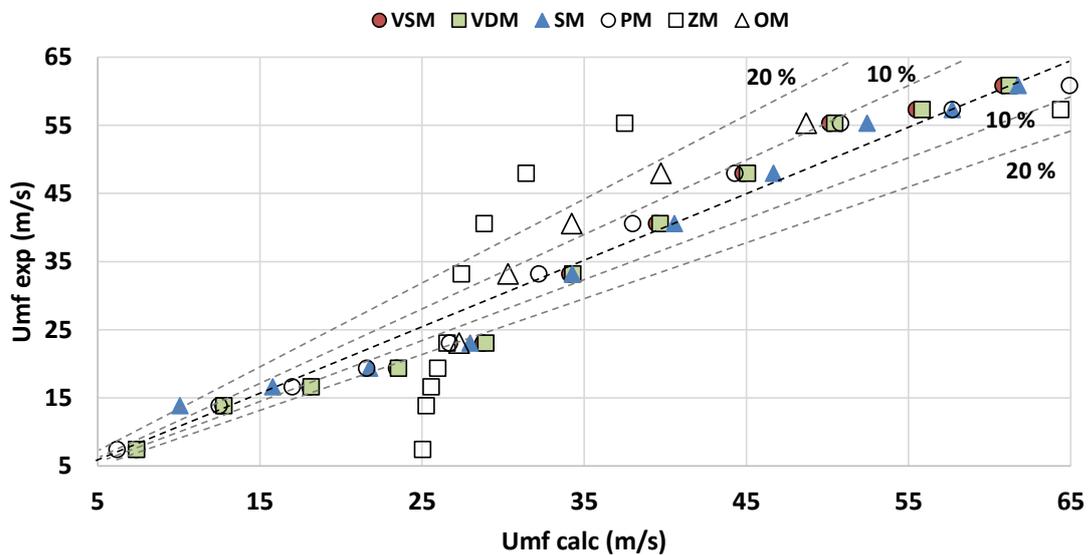
Source: Authors.

Figure 9 - Experimental versus calculated minimum fluidization velocity for WS and sand mixtures.
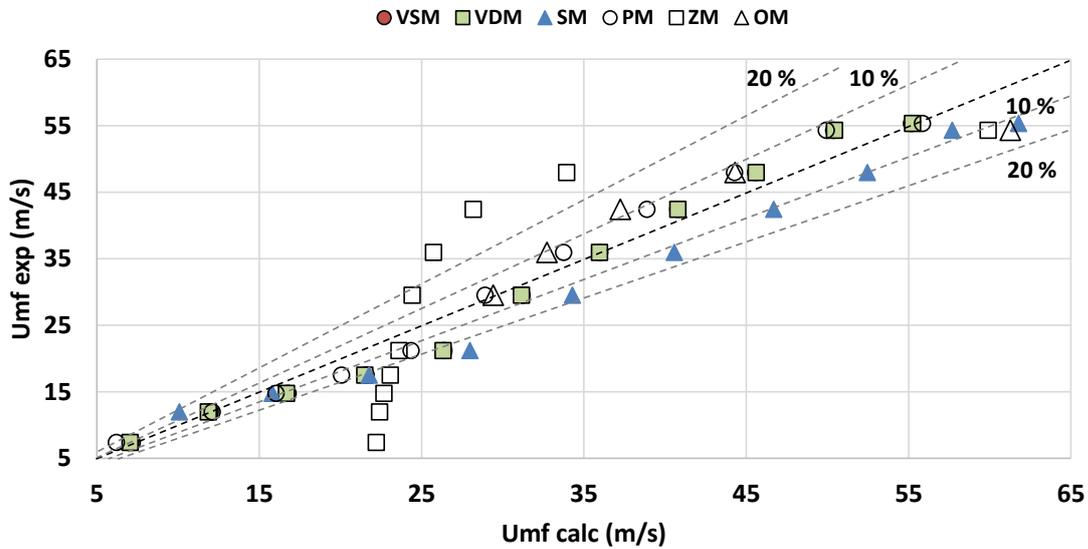
Source: Authors.

Figure 10 - Experimental versus calculated final fluidization velocity for SR and sand mixtures.
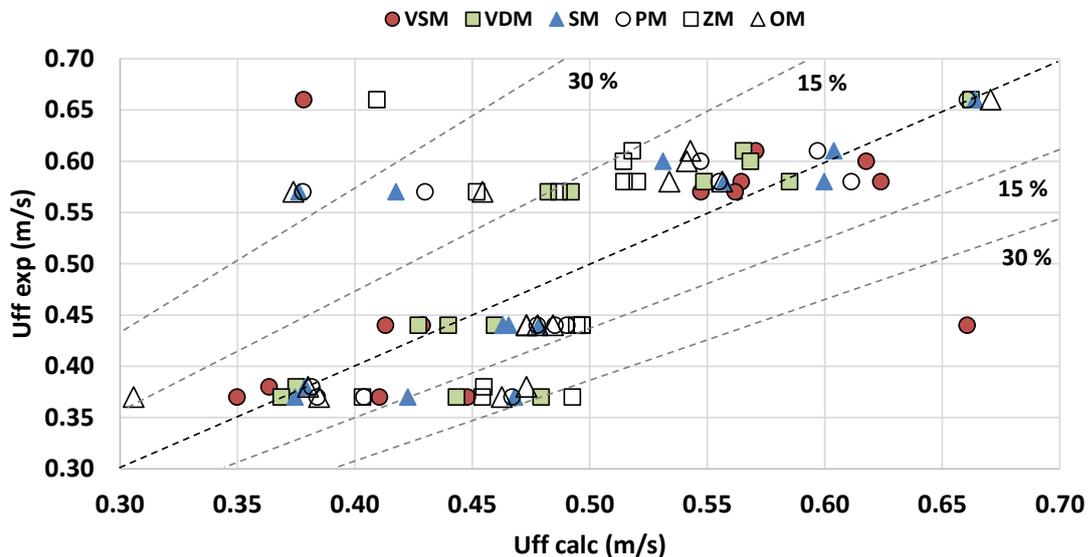
Source: Authors.

From the predicted fluidization velocity behavior as a function of the experimental fluidization velocity, the studied models were evaluated (Figs. 2–10). The results indicated a significant influence of the binary mix quality and the type of model used. Given these facts,

the contributions of the models in the prediction of fluidization velocity were evaluated considering two extreme cases of binary fluidization: two homogeneous (Figure 11) and one with segregation (Figure 12). SH and CC were used as representatives of homogeneous fluidization, and from the influence of the variables of the studied models, eight tests referring to SH and sand were performed. In these cases, the molar fraction of the biomass was 5%, 10%, and 15%; the diameter of the biomass was 0.0003, 0.0006, and 0.0008 m; and the biomass density was 1432, 1440, and 1448 kg m^{-3}; and the sand diameter and density remained constant (0.00035 m and 2695.5 kg m^{-3}). Figure 11 shows that all predicted fluidization velocities were very close to the experimental ones, even in the low segregation fluidization situation (dbio/dsand = 0.86). Most models presented relatively small parameter values (Table 4), which emphasize the importance of each variable. However, OM, VDM, and VSM presented, respectively, high values for C2, C1 and C2, and C6. The high value for C2 of OM is attributable to a decrease in the importance of the relative effective density term. The high values of C1 and C2 of VDM show a reduction in the importance of relative diameters and densities, as well as the modified Archimedes number. The high value of C6 of VSM compensates for the low values of dsand².

Figure 11 - Experimental versus calculated minimum fluidization velocity (homogeneous binary fluidization). (a) SH and sand mixtures; (b) CC and sand mixtures.
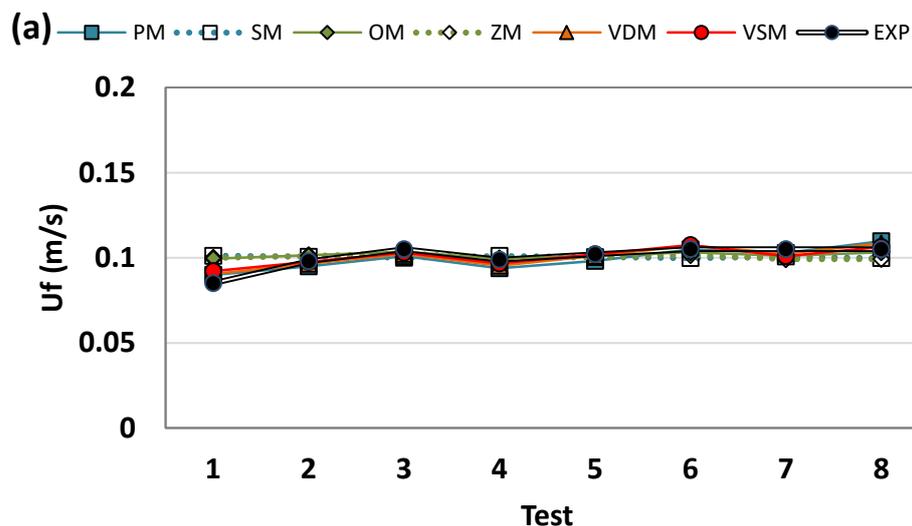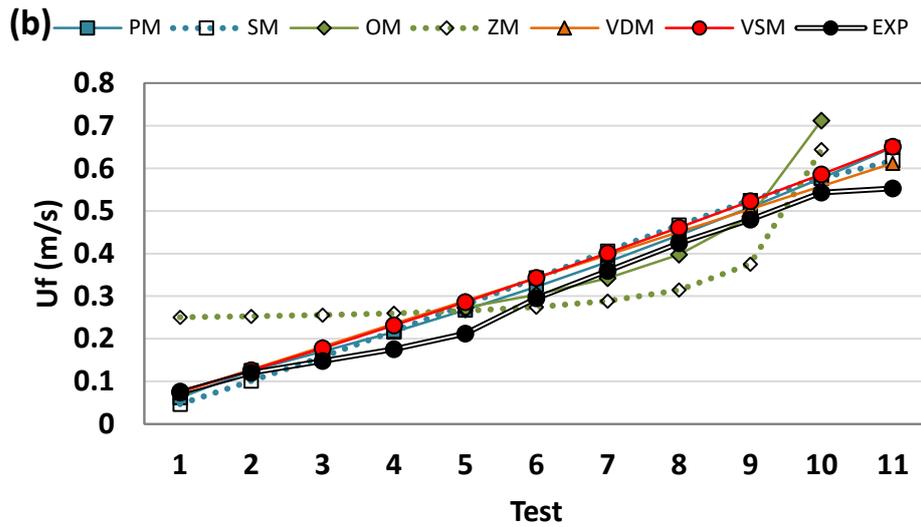
Source: Authors

The fact that SH tests were performed with low biomass mass fraction may have caused small variations in the experimental and predicted fluidization velocities. Eleven tests were performed with the homogeneous mixture containing CC (Table 5), with the biomass mass fraction varying from 0 to 1, with 10% intervals, while maintaining the other properties constant, to enlarge the effects of mass fractions of biomass on fluidization rate (Figure 11(b)).

Table 5 - Material properties of each test: CC, SH, and WT*.

Biomass	Test	W_{bio} (%)	d_{bio}	d_{sand}	ρ_{bio} (kg.m^{-3})	ρ_{sand} (kg.m^{-3})	d_{bio}/d_{sand}	ρ_{bio}/ρ_{sand}
CC	1	0.00	0.0010	0.00024	1080.0	2630.0	4.32	0.41
	2	0.10	0.0010	0.00024	1080.0	2630.0	4.32	0.41
	3	0.20	0.0010	0.00024	1080.0	2630.0	4.32	0.41
	4	0.30	0.0010	0.00024	1080.0	2630.0	4.32	0.41
	5	0.40	0.0010	0.00024	1080.0	2630.0	4.32	0.41
	6	0.50	0.0010	0.00024	1080.0	2630.0	4.32	0.41
	7	0.60	0.0010	0.00024	1080.0	2630.0	4.32	0.41
	8	0.70	0.0010	0.00024	1080.0	2630.0	4.32	0.41
	9	0.80	0.0010	0.00024	1080.0	2630.0	4.32	0.41
	10	0.90	0.0010	0.00024	1080.0	2630.0	4.32	0.41
	11	1.00	0.0010	0.00024	1080.0	2630.0	4.32	0.41
SH	1	0.05	0.0008	0.00035	1432.0	2695.5	2.29	0.53
	2	0.10	0.0008	0.00035	1432.0	2695.5	2.29	0.53
	3	0.15	0.0008	0.00035	1432.0	2695.5	2.29	0.53
	4	0.05	0.0006	0.00035	1440.0	2695.5	1.71	0.53
	5	0.10	0.0006	0.00035	1440.0	2695.5	1.71	0.53
	6	0.15	0.0006	0.00035	1440.0	2695.5	1.71	0.53
	7	0.05	0.0003	0.00035	1448.8	2695.5	0.86	0.54
	8	0.10	0.0003	0.00035	1448.8	2695.5	0.86	0.54
WT*	1	0.05	0.0006	0.00113	1301.7	2695.5	0.53	0.48
	2	0.10	0.0006	0.00113	1301.7	2695.5	0.53	0.48
	3	0.15	0.0006	0.00113	1301.7	2695.5	0.53	0.48
	4	0.05	0.0004	0.00113	1382.0	2695.5	0.31	0.51
	5	0.10	0.0004	0.00113	1382.0	2695.5	0.31	0.51
	6	0.15	0.0004	0.00113	1382.0	2695.5	0.31	0.51
	7	0.05	0.0003	0.00113	1431.4	2695.5	0.22	0.53
	8	0.10	0.0003	0.00113	1431.4	2695.5	0.22	0.53
	9	0.05	0.0006	0.00085	1301.7	2695.5	0.71	0.48
	10	0.10	0.0006	0.00085	1301.7	2695.5	0.71	0.48
	11	0.15	0.0006	0.00085	1301.7	2695.5	0.71	0.48
	12	0.05	0.0004	0.00085	1382.0	2695.5	0.41	0.51
	13	0.10	0.0004	0.00085	1382.0	2695.5	0.41	0.51
	14	0.15	0.0004	0.00085	1382.0	2695.5	0.41	0.51
	15	0.05	0.0003	0.00085	1431.4	2695.5	0.29	0.53
	16	0.10	0.0003	0.00085	1431.4	2695.5	0.29	0.53
	17	0.05	0.0006	0.00067	1301.7	2695.5	0.90	0.48
	18	0.10	0.0006	0.00067	1301.7	2695.5	0.90	0.48
	19	0.15	0.0006	0.00067	1301.7	2695.5	0.90	0.48
	20	0.05	0.0004	0.00067	1382.0	2695.5	0.52	0.51
	21	0.10	0.0004	0.00067	1382.0	2695.5	0.52	0.51
	22	0.15	0.0004	0.00067	1382.0	2695.5	0.52	0.51
	23	0.05	0.0003	0.00067	1431.4	2695.5	0.37	0.53

Data obtained from Paudel and Feng (2013) (CC) and Oliveira et al. (2013) (SH and WT*)

In this case, all models, except for ZM, could follow the growth trend of experimental

fluidization velocity. In general, an increase in the biomass mass fraction caused the parameters to increase in all models. However, the high value of C1 of ZM was responsible for the almost linear behavior of fluidization velocity, up to 70% of the biomass in the mixture. From this value, fluidization velocity tended to increase. Similar behavior also occurred with OM between 80% and 90% of biomass; however, C2 of the relative effective density term indicated that the predicted fluidization velocities had good approximations of the experimental values between 0% and 90% of the biomass.

The results showed in Figure 11 indicate that the high relative diameter of CC (4.32) for any biomass fraction and relatively small SH fractions (up to 15%), regardless of the relative diameter (2.29, 1.71, and 0.86), contributes to the fact that most models predict the fluidization velocity for homogeneous mixtures relatively accurately.

Model behaviors for segregated mixtures were evaluated from Figure 12. The chosen mixture was WT*, whose properties were defined for 23 tests (Table 5). In this case, the mass fractions and sand density were equal to those considered for SH, but the biomass diameters were similar (0.0003, 0.0004, and 0.0006 m), the sand diameters were larger (0.00067, 0.00085, and 0.00113 m), and biomass densities were lower (1301.7, 1382.0, and 1431.4 kg m^{-3}). Therefore, the relative diameters were low (0.22, 0.29, 0.31, 0.37, 0.41, 0.52, 0.53, 0.71, 0.86, and 0.90) and at intermediate relative densities (0.48, 0.51, and 0.53). Figure 12(a) shows the behaviors of VDM and VSM throughout the 23 tests. These models predicted fluidization velocity values close to the experimental values until test 11. In this case, the decrease in relative diameter followed that in the predicted fluidization velocity. From test 8 to test 9, there was a relative density inversion from 0.22 to 0.71, which contributed to an increase in fluidization velocity. However, from test 9 to test 11, the fluidization velocity decreased, due to an increase in the biomass mass fraction. This result is contradictory to that concluded in Figure 11(b); however, the behavior changed due to a greater segregation of tests from 9 to 11 (0.71) compared to SH (1.71).

Figure 12 - Experimental versus calculated minimum fluidization velocity for WT* and sand mixtures (binary fluidization with segregation). (a) VSM and VDM; (b) SM and PM; (c) OM and ZM.
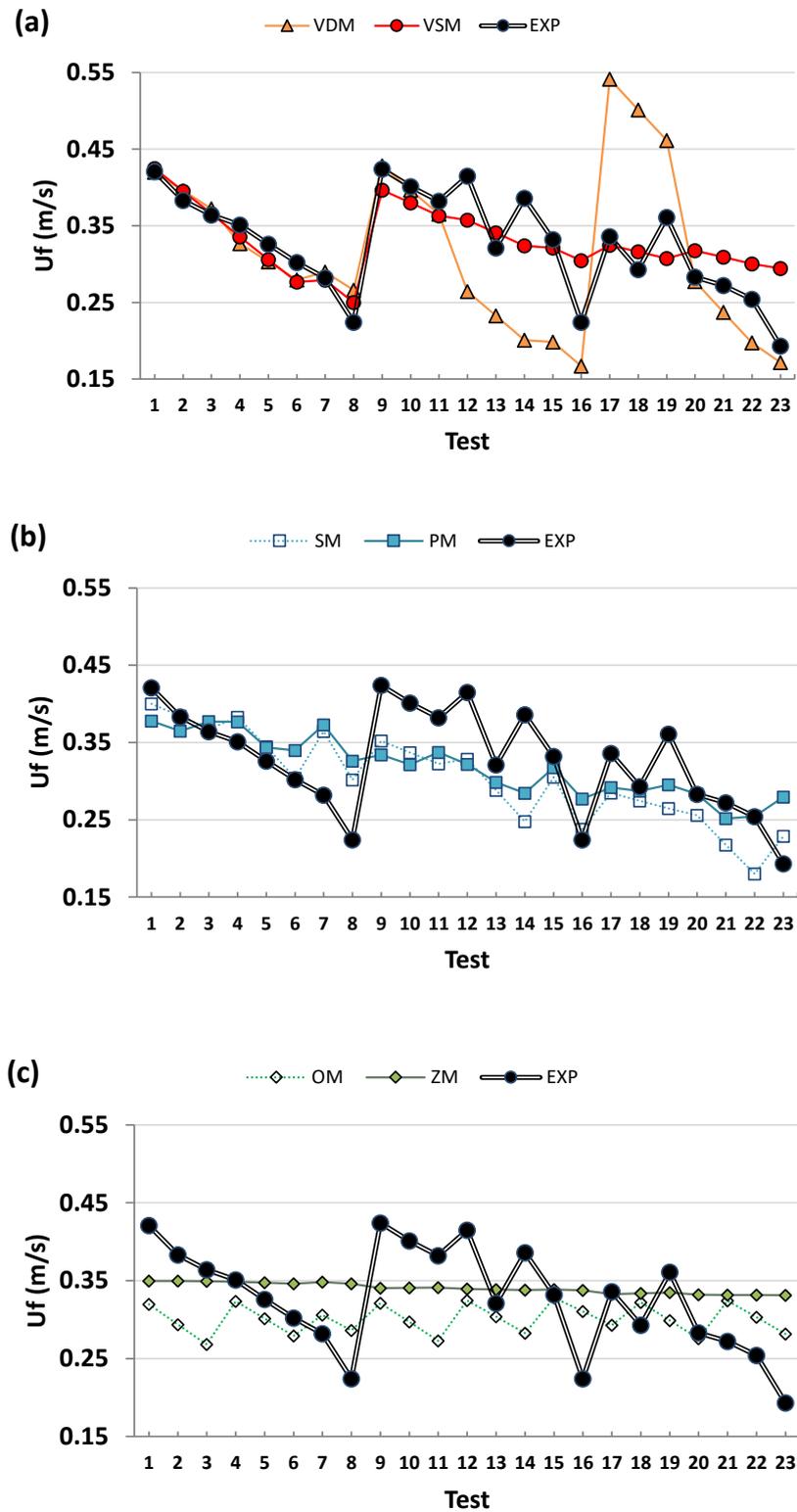
Source: Authors.

Despite the variations in material properties, the predictions also followed the experimental values until test 11 (Figure 12(a)). From test 12, neither model obtained good predictions in relation to the experimental data presented by Oliveira et al. (2013), mainly because tests 12, 14, 15, 17, and 18 did not follow the same logic as that presented in tests 1–11. As tests 1 to 11 showed decreasing and increasing fluidization velocities, depending on the decrease or increase in relative diameter, the same behaviors should have occurred for tests 12–16 and 17–23. This behavior can be better explained by comparing the property values of tests 4–6 with those of tests 12–14 or comparing tests 9–11 with tests 17–19. These tests had low values of relative diameter and percentage of increasing biomass, so the behaviors of all of them should be decreasing as a function of segregation. If so, VDM and VSM can better predict the system behavior. VDM presented high values of C1–C4, showing that the relative diameter and relative density had a small influence on fluidization velocity. Similar results were obtained with VSM, whose properties had small relevance in determining fluidization velocity.

Figure 12(b) shows the behaviors of SM for the 23 assays with a segregated mixture. The fluidization velocities calculated from these models also followed the behavior of the experimental values, taking as reference the discussions already conducted. PM had high value of C1–C3, which implies a decrease in the importance of the Archimedes number and the mass fractions of the materials. SM had high values of C1 and C2, both related to the decreased importance of the Archimedes number. Overall, these models had similar behaviors in all tests, and therefore, the only difference between them (parameters H for PM and C2 for SM) was reduced due to the high parameter values.

Figure 12(c) shows the behaviors of OM and ZM for the segregated mixtures. The fluidization velocities calculated from these models did not follow the trend of experimental velocity. ZM was insensitive to predicting practically constant fluidization velocities, even with variations in the properties of the materials and the fluidizing medium. The parameter values of this model were very low, but this was insignificant because this model did not fit well with the segregated mixtures. OM was not insensitive to variations in material properties; however, its results showed a standardized behavior incompatible with the experimental results. As in ZM, OM presented parameters with low values and seems inadequate to predict the fluidization velocity of segregated systems.

In general, the primary source of error in the predictions made by the studied models occurs when working with segregated systems. No model produced results that wholly followed variations of the real values in all tests. Therefore, the choice of the most suitable

models for the prediction of the fluidization velocity will be made by measuring the average discrepancy between the experimental and calculated values (δ (%)). The average discrepancies considering all tests of a specific biomass are shown in Figure 13.

Figure 13 - Fluidization velocity discrepancy for individual regression.
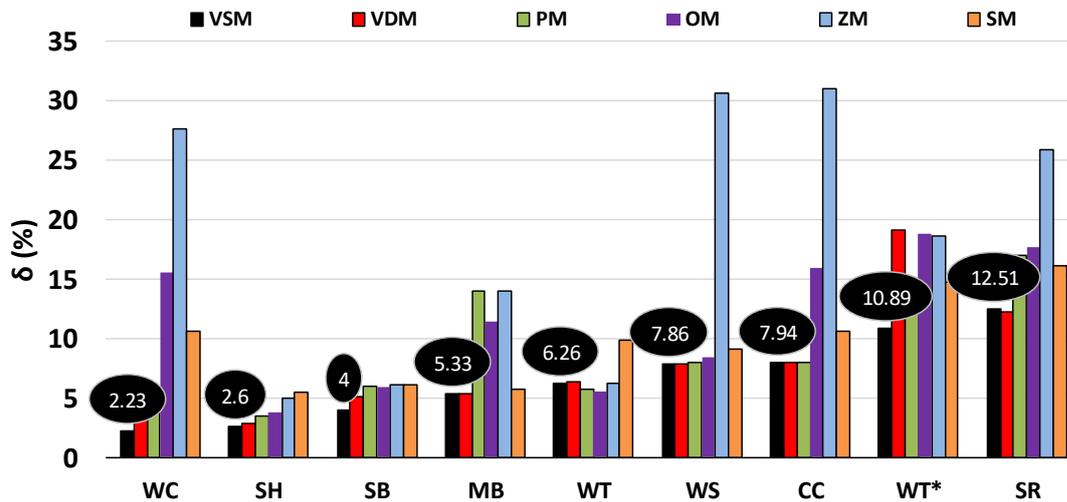
Source: Authors.

Assuming the choice of the best models among those researched, Figure 13 offers an overview of their behaviors for each biomass. Most of the models provided reasonable predictions of the minimum fluidization velocity, but the most significant discrepancy values involving all models were obtained for WT* and SR. These were the biomasses with parameters and differentiated characteristics, as previously explained. ZM exhibited the lowest performance, because it did not adequately predict the experimental fluidization velocities for WC, MB, WS, CC, WT*, and SR.

The models that showed the lowest discrepancy values for most biomasses were VSM, VDM, and PM. The importance of these models concerning the fluidization systems treated in this study involves broad fluidization situations, with highly homogeneous mixtures and severe segregation. In general, OM and SM did not show good performance because they did not perform well in situations with segregation and involving Geldart D classification of materials. ZM seemed to be limited by exponent 1.23, whose performance has been undermined because its predictions are not related to the homogeneity or segregation of the mixture.

VDM and PM were developed based on Reynolds and Archimedes numbers (modified

and unmodified). In the calculations of fluidization velocity, eight properties of the materials and gas were considered: sand and biomass diameters; densities of sand, biomass, and air; mass fraction of biomass; acceleration of gravity; and viscosity of air. On the other hand, VSM did not have dimensionless terms that gave physical meaning to the fluidization phenomenon, which is comparatively simpler, considering only three material properties: sand and biomass diameters and biomass fraction. Besides considering fewer properties, VSM also obtained very low discrepancy values for all biomasses and fluidization situations, contrasting with the performance of the other models, even under more severe fluidization conditions (Figure 13).

4. Final Considerations

The efficiencies of VSM, VDM, PM, ZM, SM, and OM were estimated to predict the minimum fluidization velocity of biomasses--WT, SB, SH, WC, MB, CC, and WS--and final fluidization velocity of SR.

Initially, it was verified that the minimum fluidization velocities predicted from the models fitted the experimental data of each biomass (WT, WT*, SB, or SH) showed lower discrepancy values than those predicted by models that had their parameters adjusted to from the biomass dataset (WT + WT* + SB + SH). In all these cases, the smallest discrepancies were obtained when the model parameter predictions were made from the data of each biomass; this procedure seems to be necessary for a good prediction. Research on the performance of VSM, VDM, PM, OM, ZM, and SM involved binary fluidization systems with sand and nine biomasses, giving a broader character to the use of these models. VSM produced dispersions mostly below 10% and average discrepancies between 2.23% and 12.51%. Despite the importance shown by VDM, VSM was the most robust among the models we studied. This model made good predictions for homogeneous fluidization systems as well as for segregated systems. VSM exhibits an extra advantage of having in its structure only material diameters and biomass mass fraction as independent variables. The reduction in the number of variables of VSM concerning the other models causes a decrease in computational effort, and simplifies the information needed to perform fluidization velocity prediction.

Despite the highlight of VSM, this study was based on the final fluidization velocity calculation of binary mixtures of sand and biomass. These mixtures are typical of a pyrolysis bed that produces bio-oil. However, in a real system, the biochar produced in the reaction

remains in the bed during pyrolysis. Then, the fluidization evaluation of a mixture of sand, sisal residue, and biochar should be part of future studies, as well as the determination of a new mathematical correlation that physically describes the behavior of the operational variables in the final fluidization velocity of a ternary mixture.

Acknowledgment

Nomenclature

Ar^* – Archimedes number modified

d_{bio} – biomass particle size, mm

dp_{eff} – effective particle size, mm

d_{sand} – sand particle size, mm

g – acceleration of gravity, m s^{-2}

Re_{ff}^* – Reynolds number modified

u_f – fluidization velocity, m s^{-1}

u_{mf} – minimum fluidization velocity, m s^{-1}

u_{ff} – final fluidization velocity, m s^{-1}

w_{bio} – biomass mass fractions

w_{sand} – sand mass fractions

φ – discrepancy, %

δ – average discrepancy, %

ρ_{bio} – biomass density, kg m^{-3}

ρ_{eff} – effective density of the mixture, kg m^{-3}

ρ_f – density of fluidizing medium, kg m^{-3}

ρ_{sand} – sand density, kg m^{-3}

μ – viscosity of the fluidizing gas, kg.m^{-1} s^{-1}

References

Broyden, C. G. (1967). Quasi-Newton methods and their application to function minimisation.. Mathematics. Computation. 21, 368–381. MR 0224273, https://doi.org/10.1090/S0025-5718-1967-0224273-2.

Bridgwater, A. V. (2004). Biomass fast pyrolysis - Review paper. Thermal Sciences, 8 (2), 21-49.

Chiba, S., Chiba, T., Nienow, A. W., & Kobayashi, H. (1979). The minimum fluidization velocity bed expansion and pressure drop profile of binary particle mixtures. Powder Technology, 22, 255-269.

Formisani, B., Girimonte, R. (2003). Experimental analysis of the fluidization process of binary mixtures of solids. Kona, 21, 66-75.

Formisani, B., Girimonte, R., & Vivacqua, V. (2011). Fluidization of mixtures of two solids differing in density or size. American Institute of Chemical Engineers Journal, 57 (9), 2325-2333.

Formisani, B., Girimonte, R., & Vivacqua, V. (2013). Fluidization of mixtures of two solids: a unified model of the transition to the fluidized state. American Institute of Chemical Engineers Journal, 59 (3), 729-735.

Hooke, R., Jeeves, T. A. (1961). Direct search solution of numerical and statistical problems. Journal Association Computing Machinery., 8, 212-229.

Jeong, J-Y., Lee, U-D., Chang, W-S., & Jeong, S-H. (2016). Production of bio-oil rich in acetic acid and phenol from fast pyrolysis of palm residues using a fluidized bed reactor: Influence of activated carbons. Bioresource Technology, 219, 357–364.

Oliveira, T. J. P., Cardoso, C. R., & Ataíde, C. H. (2013). Bubbling fluidization of biomass and sand binary mixtures: Minimum fluidization velocity and particle segregation. Chemical Engineering and Processing, 72, 113-121.

Paudel, B., & Feng, Z-G. (2013). Prediction of minimum fluidization velocity for binary mixtures of biomass and inert particles. Powder Technology, 237, 134-140.Yang, W. (2003). Handbook of Fluidization and Fluid-Particle Systems. Edited by Wen-Ching Yang, 12-38.

Rao, T. R., Bheemarasetti, J. V. R. (2001). Minimum fluidization velocities of mixtures of biomass and sands. Energy, 26, 633–644.

Rosenbrock, H. H. (1960). An automatic method for finding the greatest or least value of a function. Computer Journal, 3, 175-184.

Si, C., & Guo, Q. (2008). Fluidization Characteristics of Binary Mixtures of Biomass and Quartz Sand in an Acoustic Fluidized Bed. Industrial & Engineering Chemistry Research, 47, 9773–9782.

Vasconcelos, D., Batalha, G., Pereira, L. G., & Pires, C. A. (2018). Fluidization for Binary Mixtures of Sisal Residue and Sand: A New Model for Deriving the Final Fluidization Velocity. Particuology, 40, 10–22.

Wang, F., Zeng, X., Wang, Y., Su, H., Yu, J., & Xu, G. (2016). Non-isothermal coal char gasification with CO_2 in a micro fluidized bed reaction analyzer and a thermogravimetric analyzer. Fuel, 164, 403–409.

Wen, C. Y., & Yu, Y. H. (1966). A generalized method for predicting minimum fluidization velocity. American Institute of Chemical Engineers, 12, 610-612.

Yang, W. C. (2003). Handbook of fluidization and fluid-particle systems. 12–38. Boca Raton: CRC press.

Zhong, W., Jin, B., Zhang, Y., Wang, X., & Xiao, R. (2008). Fluidization of biomass particles in a gas–solid fluidized bed. Energy Fuels, 22, 4170–4176.

Percentage of contribution of each author in the manuscript

David da Silva Vasconcelos – 30%

Sirlene Barbosa Lima – 10%

Ana Cristina Morais da Silva – 10%

José Mário Ferreira Júnior – 20%

Carlos Augusto de Moraes Pires – 30%

Percentage of contribution of each author in the manuscript